From Core/Shell Structured FePt/Fe_3O_4/MgO to Ferromagnetic FePt Nanoparticles

Jaemin Kim,[†] Chuanbing Rong,[‡] Youngmin Lee,[†] J. Ping Liu,[‡] and Shouheng Sun*[,†]

Department of Chemistry, Brown University, Rhode Island 02912, and Department of Physics, University of Texas at Arlington, Arlington, Texas 76019

Received September 13, 2008. Revised Manuscript Received October 6, 2008

This paper reports an improved synthesis of hard magnetic fct-FePt nanoparticles (NPs) from reductive annealing of fcc-FePt/Fe_3O_4/MgO NPs followed by MgO removal. The fcc-FePt/Fe_3O_4 NPs are made by a one-pot reaction of $Pt(acac)_2$ with $Fe(CO)_5$ in the presence of oleic acid and oleylamine and are coated with a layer of MgO via the thermal decomposition of $Mg(acac)_2$. The MgO coating prevents FePt from sintering under high temperature reductive annealing conditions. The fct-FePt NPs obtained from the 650 °C annealing of the fcc-FePt/Fe_3O_4/MgO NPs show a coercivity value of 2 T at 300 K, suitable for various nanomagnetic applications.

Introduction

Magnetic iron−platinum (FePt) nanoparticles (NPs) made from solution phase chemical syntheses have shown great potential for high performance permanent magnet,[1−3] high density data storage,[4−6] and highly efficient biomedicine applications.[7−9] Their magnetic properties can be tuned not only by NP sizes but also by Fe, Pt composition and Fe, Pt atomic arrangement in the FePt alloy structure. Due to the high magnetocrystalline anisotropy and robust chemical stability, face-centered tetragonal (fct) FePt NPs are particularly interesting as models for nanomagnetism study[10,11] and as building blocks for constructing single NP information storage media.[4−6] The fct-FePt NPs are commonly made by annealing face centered cubic (fcc) FePt NPs at high temperatures, usually >550 °C.[12−14] But this high temperature annealing also results in various degrees of NP aggregation and sintering, deteriorating the quality of NP arrays. To avoid this aggregation/sintering problem, FePt NPs are either coated with SiO_2[15,16] or MgO[17] or grinded with a large excess of NaCl[18,19] before high temperature annealing is applied. The controlled MgO coating is especially interesting as it not only protects FePt NPs from sintering at temperatures up to 800 °C[17] but also provides a model system for studying magnetic tunneling between FePt NPs with potentially much higher magneto-resistance than the thin film structure.[20] Further, the MgO shell can be removed readily by a dilute acid washing, giving either fcc-FePt or fct-FePt NPs with minimum surface contamination for catalytic applications.[21−23]

Here we report an improved approach to fct-FePt NPs and their hexane dispersion via reductive annealing of FePt/Fe_3O_4/MgO followed by MgO removal. In the FePt/MgO NP system reported previously,[17] the robust MgO coating is found to limit the mobility of the Fe, Pt atoms in the FePt structure, making the fcc to fct conversion so difficult that even at 750 °C for 6 h, the FePt structure is not fully fct-ordered. In the current approach, the Pt-rich fcc-FePt/Fe_3O_4 NPs were first made and coated with a thin layer of MgO. The FePt/Fe_3O_4/MgO NPs were then reduced by Ar + H_2 (5%). Due to the interfacial diffusion between Pt and Fe, well-ordered fct-FePt NPs were obtained at 650 °C for 6 h,

* Corresponding author. E-mail: ssun@brown.edu.
† Brown University.
‡ University of Texas at Arlington.

(1) Kneller, E. F.; Hawig, R. *IEEE Trans. Magn.* **1991**, *27*, 3588–3600.
(2) Skomski, R.; Coey, J. M. D. *Phys. Rev. B* **1993**, *48*, 15812–15816.
(3) Zeng, H.; Li, J.; Wang, Z. L.; Liu, J. P.; Sun, S. *Nature* **2002**, *420*, 395–398.
(4) Weller, D.; Doerner, M. F. *Annu. Rev. Mater. Sci.* **2000**, *30*, 611–644.
(5) Sun, S.; Murray, C. B.; Weller, D.; Folks, L.; Moser, A. *Science* **2000**, *287*, 1989–1992.
(6) Moser, A.; Takano, K.; Margulies, D. T.; Albrecht, M.; Sonobe, Y; Ikeda, Y.; Sun, S.; Fullerton, E. E. *J. Phys. D: Appl. Phys* **2002**, *35*, R157–R167.
(7) Pankhurst, Q. A.; Connolly, J.; Jones, S. K.; Dobson, J. *J. Phys. D: Appl. Phys.* **2003**, *36*, R167−R181.
(8) Sun, S. *Adv. Mater.* **2006**, *18*, 393–403.
(9) Gao, J.; Liang, G.; Cheung, J. S.; Pan, Y.; Kuang, Y.; Zhao, F.; Zhang, B.; Zhang, X.; Wu, E. X.; Xu, B. *J. Am. Chem. Soc.* **2008**, *130*, 11828–11833.
(10) Ulmeanu, M.; Antoniak, C.; Wiedwald, U.; Farle, M.; Frait, Z.; Sun, S. *Phys. Rev. B* **2004**, *69*, 054417.
(11) Antoniak, C.; Lindner, J.; Spasova, M.; Sudfeld, D.; Acet, M.; Farle, M.; Fauth, K.; Wiedwald, U.; Boyen, H.-G.; Ziemann, P.; Wilhelm, F.; Rogalev, A.; Sun, S. *Phys. Rev. Lett.* **2006**, *97*, 117201.
(12) Dai, Z. R.; Sun, S.; Wang, Z. L. *Nano Lett.* **2001**, *1*, 443–447.
(13) Elkins, K. E.; Vedantam, T. S.; Liu, J. P.; Zeng, H.; Sun, S.; Ding, Y.; Wang, Z. L. *Nano Lett.* **2003**, *3*, 1647–1649.
(14) Vedantam, T. S.; Liu, J. P.; Zeng, H.; Sun, S. *J. Appl. Phys.* **2003**, *93*, 7184–7186.
(15) Yamamoto, S.; Morimoto, Y.; Ono, T.; Takano, M. *Appl. Phys. Lett.* **2005**, *87*, 032503.
(16) Tamada, Y.; Yamamoto, S.; Takano, M.; Nasu, S.; Ono, T. *Appl. Phys. Lett.* **2007**, *90*, 162509.
(17) Kim, J.; Rong, C.; Liu, J. P.; Sun, S. *Adv. Mater.* **2008**, in press.
(18) Li, D.; Poudyal, N.; Nandwana, V.; Jin, Z.; Elkins, K; Liu, J. P. *J. Appl. Phys.* **2006**, *99*, 08E911.
(19) Rong, C.; Poudyal, N.; Chaubey, G. S.; Nandwana, V.; Liu, Y.; Wu, Y. Q.; Kramer, M. J.; Kozlov, M. E.; Baughman, R. H.; Liu, J. P. *J. Appl. Phys.* **2008**, *103*, 07E131.
(20) Parkin, S. S. P.; Kaiser, C.; Panchula, A.; Rice, P. M.; Hughes, B.; Samant, M.; Yang, S. *Nat. Mater.* **2004**, *3*, 862–867.
(21) Chen, W.; Kim, J.; Xu, L.; Sun, S.; Chen, S. *J. Phys. Chem. C* **2007**, *111*, 13452–13459.
(22) Chen, W.; Kim, J.; Sun, S.; Chen, S. *Langmuir* **2007**, *23*, 11303–11310.
(23) Chen, W.; Kim, J.; Sun, S.; Chen, S. *J. Phys. Chem. C* **2008**, *112*, 3891–3898.

10.1021/cm8024878 CCC: $40.75
Published on Web 11/06/2008

100 °C lower than that for the formation of fct-FePt from the fcc-FePt/MgO NPs. In the FePt/Fe_3O_4/MgO structure, the Fe_3O_4 shell thickness was used to control the final FePt composition. For example, the 12 nm fct-$Fe_{52}Pt_{48}$ NPs were synthesized by annealing 7 nm/2.5 nm fcc-FePt/Fe_3O_4/MgO NPs. Their coercivity reached 3.2 T at 5 K and 2 T at 300 K. They could be stabilized by hexadecanethiol and oleic acid and redispersed in hexane by the MgO removal and NP extraction process.[17] The FePt NPs prepared in this work are suitable for various nanomagnetic and catalytic applications.

Experimental Section

Chemicals. Iron pentacarbonyl (98%), oleic acid (OA) (90%), oleylamine (OAm) (>70%), 1-octadecene (90%), and 1,2-tetradecanediol (98%) were purchased from Aldrich. Platinum(II) acetylacetonate, $Pt(acac)_2$ (98%), and magnesium(II) acetylacetonate, $Mg(acac)_2$ (98%), were purchased from Strem. Hydrochloric acid was purchased from EMD chemicals. All syntheses were carried out under a standard airless condition using the Schlenk line. The commercially available reagents were used without further purification.

Synthesis of FePt/Fe_3O_4 NPs. To get ~12 nm FePt/Fe_3O_4 NPs by one-pot synthesis, 0.5 mmol of $Pt(acac)_2$, 4 mmol of OA, and 4 mmol of OAm were mixed with 10 mL of 1-octadecene under gentle argon gas flow. The mixture was heated up to 120 °C, and 0.20 mL of $Fe(CO)_5$ was added under the blanket of argon gas. The solution was heated to 240 °C for 30 min to ensure decomposition of $Fe(CO)_5$ and growth of FePt NPs and followed by refluxing and short time air oxidation at 320 °C for 30 min. The heating source was removed, and the solution was cooled down to room temperature. The black product was precipitated by adding 40 mL of absolute ethanol and separated by centrifugation. The dark yellow supernatant was discarded, and the precipitate was dispersed in 15 mL of hexane. By adding 20 mL of ethanol, the NPs were precipitated out again and centrifuged. This procedure was repeated for two more times. Finally, the product (~200 mg) was redispersed in 10 mL of hexane in the presence of 0.05 mL of each of OA and OAm.

Synthesis of FePt/Fe_3O_4/MgO NPs. FePt/Fe_3O_4/MgO NPs were synthesized by the following procedure. First, 2 mmol of $Mg(acac)_2$, 4 mmol of 1,2-tetradecanediol, and 4 mmol of OA and 4 mmol of OAm were put into the four-neck flask containing 20 mL of benzyl ether. Then, the vigorously stirred solution was heated to 80 °C and kept for 5 min to dissolve the mixture completely under a gentle nitrogen gas flow. A total of ~100 mg of the as-synthesized FePt/Fe_3O_4 NPs dispersed in 5 mL of hexane was added quickly into the flask within ~2 s. The solution was heated to 120 °C and kept at this temperature for 20 min to ensure hexane was evaporated. Under the blanket of nitrogen gas, the solution was heated to 298 °C and was refluxed for 1 h. Finally, the heating source was removed and the solution was cooled down to room temperature. The FePt/Fe_3O_4/MgO NPs were separated and purified by using hexane and ethanol and centrifugation as described in the synthesis of FePt/Fe_3O_4 NPs. Finally, the NPs were kept in 10 mL of hexane.

Synthesis of fct-FePt NPs from the FePt/Fe_3O_4/MgO NPs. To make ferromagnetic FePt NPs, the FePt/Fe_3O_4/MgO NPs powder was put in a porcelain combustion boat and annealed at temperatures from 550 to 800 °C and the optimum annealing condition was found to be 650 °C for 6 h. After cooled down, the magnetic powder was characterized. To make FePt NP hexane dispersion, the annealed FePt/MgO powder was transferred into a vial. The diluted HCl solution (<10% vol) and hexane containing both HDT and OA were added into the vial. The suspension was sonicated for ~10 s and shaken for ~10 min. The FePt NPs stabilized by HDT and OA were extracted and dispersed in hexane.

Scheme 1. Synthesis of Pt-Rich FePt/Fe_3O_4/MgO NPs and fct-FePt/MgO NPs

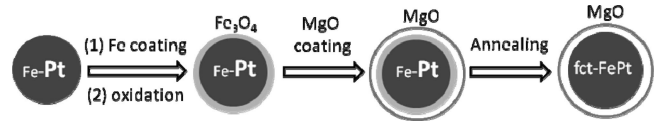

FePt NP Characterization. The samples for transmission electron microscopy (TEM) images were prepared by depositing the hexane dispersion of the NPs on the amorphous carbon-coated copper grids. The NP samples for high temperature annealing were prepared on carbon type-A copper grid. TEM images were acquired on a Philips EM 420 at 120 kV and HRTEM images were obtained on a JEOL 2010 at 200 kV. The Fe and Pt composition of the FePt NPs were measured by Oxford energy-disperse X-ray spectroscopy. The powder X-ray diffraction (XRD) patterns of the samples were collected on Bruker AXS D8-Advance diffractometer with Cu Kα radiation (λ = 1.5418 Å). Magnetic studies were performed on a Quantum Design Superconducting Quantum Interface Device (SQUID) with a field up to 70 kOe. The samples for diffraction and magnetic measurements were deposited on Si substrates.

Results and Discussion

Synthesis of FePt/Fe_3O_4 and FePt/Fe_3O_4/MgO NPs. Pt-rich FePt/Fe_3O_4 NPs were synthesized from one-pot reaction of $Fe(CO)_5$, $Pt(acac)_2$, OA, and OAm in 1-octadecene. The mechanism for the formation of these Pt-rich FePt/Fe_3O_4 NPs under the current reaction conditions is similar to what has been proposed for the formation of fcc-FePt/Fe_3O_4,[24] but the process is controlled so that there is no significant diffusion of Fe into Pt in the reaction condition, as shown in Scheme 1. The Pt-rich FePt NPs are formed from the simultaneous reduction of $Pt(acac)_2$ and partial decomposition of $Fe(CO)_5$ at temperature < 240 °C. At a higher reaction temperature, more Fe atoms coat over the existing Pt-rich FePt NPs, forming Pt-rich FePt/Fe NPs that are further oxidized to Pt-rich FePt/Fe_3O_4 NPs. The amount of $Fe(CO)_5$ is optimized so that the ratio of Fe/Pt is close to 1/1. MgO is coated over the FePt-Fe_3O_4 NP surface via the direct thermal decomposition of $Mg(acac)_2$ in the condition that is similar to what has been used for the synthesis of Fe_3O_4 NPs.[25,26]

Figure 1A shows the TEM image of the as-synthesized FePt/Fe_3O_4 NPs with average total diameter of 12 nm. The core FePt NPs are in cube-like shape. Figure 1B is the HRTEM image of one representative FePt/Fe_3O_4 NP. It can be seen that the FePt is surrounded by a polycrystalline Fe_3O_4 shell. The lattice fringes of the core FePt NP are not clearly identified due to the image interference by the Fe_3O_4 shell. The elemental analysis of the core/shell structure shows Fe:Pt = 52:48.[27] Figure 1C,D shows the TEM and HRTEM images of the as-synthesized FePt/Fe_3O_4/MgO NPs. The MgO shell and Fe_3O_4 shell are not clearly distinguished due to the light electron density and the close lattice spacings of

(24) Chen, M; Liu, J. P.; Sun, S. *J. Am. Chem. Soc.* **2004**, *126*, 8394–8395.
(25) Sun, S.; Zeng, H. *J. Am. Chem. Soc.* **2002**, *124*, 8204–8205.
(26) Zeng, H.; Rice, P. M.; Wang, S. X.; Sun, S. *J. Am. Chem. Soc.* **2004**, *126*, 11458–11459.
(27) See the Supporting Information.

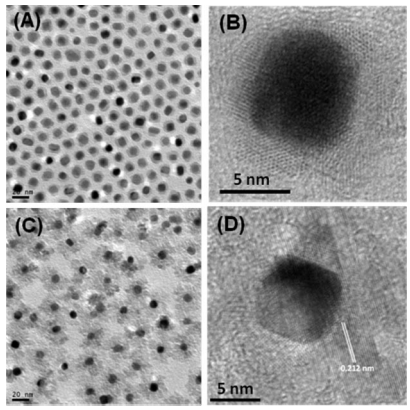

Figure 1. (A) TEM and (B) HRTEM images of the as-synthesized FePt/Fe_3O_4 NPs; (C) TEM and (D) HRTEM images of the as-synthesized FePt/Fe_3O_4/MgO NPs.

these oxides. The measured lattices with a spacing 0.212 nm could be from either MgO (200) (lattice spacing 0.211 nm) or Fe_3O_4 (400) (lattice spacing 0.209 nm).

Reductive Annealing of the Pt-Rich fcc-FePt/Fe_3O_4/MgO NPs. The Pt-rich fcc-FePt/Fe_3O_4/MgO NPs were transformed into ferromagnetic fct-FePt/MgO NPs upon reductive annealing under Ar + H_2 (5%) at high temperatures for 6 h. Hydrogen reduces Fe_3O_4 to Fe, releasing H_2O and causing defects in oxygen sites. Such defects may promote interdiffusion between Fe and Pt-rich FePt matrix, facilitating the formation of fct-FePt. This easy fct structure formation may be compared with what is observed in the ternary MFePt NPs in which different M's are doped into the FePt matrix for decreasing the fcc to fct conversion temperature.[28−36] MgO, as a coating material, is thermally robust due to its high melting point (over 2000 °C)[37,38] and stays intact at the high temperature annealing conditions, effectively protecting the FePt NPs from sintering,[27] as shown in Scheme 1. Figure 2A,B is the FePt NPs obtained from the annealing of the FePt/Fe_3O_4/MgO NPs at 650 °C for 6 h under Ar + H_2 (5%). The FePt NPs (∼12 nm) in MgO shell have no obvious overall size change compared to the as-synthesized FePt/Fe_3O_4 NPs. The HRTEM image of a single FePt/MgO NP shows that MgO is better crystallized around the FePt NP. The FePt NP lattices are not readily seen due to the MgO shell interference.

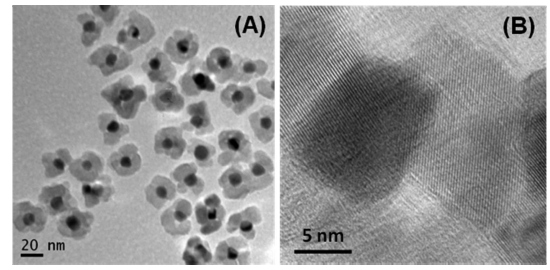

Figure 2. (A) TEM and (B) HRTEM (B) images of the FePt/MgO NPs obtained from the reductive annealing of the FePt/Fe_3O_4/MgO NPs at 650 °C for 6 h under Ar + H_2 (5%).

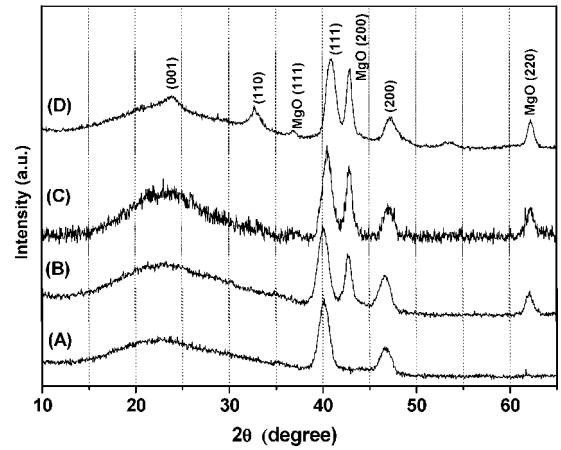

Figure 3. XRD patterns of (A) the as-synthesized FePt/Fe_3O_4 NPs and (B) the FePt/Fe_3O_4/MgO NPs before annealing and the FePt/MgO NPs obtained from annealing the MgO coated NPs at (C) 600 °C and (D) 650 °C for 6 h under Ar + H_2 (5%).

Structural Analysis on the FePt NPs. X-ray diffraction (XRD) patterns in Figure 3 show the as-synthesized FePt/Fe_3O_4 (Figure 3A) and FePt/Fe_3O_4/MgO NPs before (Figure 3B) and after the thermal annealing (Figure 3C,D) at different temperatures. The diffraction peaks from the as-synthesized Fe_3O_4 are weak due likely to its low crystallinity or thin coating. The chemically disordered fcc-FePt NPs show the typical (111) and (200) peaks in Figure 3A. The peaks around $2\theta = 43°$ and 62° in Figure 3B come from MgO. After annealing at 600 °C, the (111) and (200) peaks from the FePt NPs (Figure 3C) are shifted to the position that are ∼1° higher than that for the fcc-FePt, but the diffraction pattern does not show a clear fct phase in the FePt structure after this annealing. As the annealing temperature is increased to 650 °C, the (001) and (110) peaks emerge from the diffraction pattern (Figure 3D), indicating the formation of the fct-FePt at 650 °C. This annealing temperature is 100 °C lower than that (750 °C) needed for the fcc to fct conversion in the fcc-FePt/MgO NPs,[17] implying that diffusion between Fe and Pt-rich FePt facilitates the formation of fct-FePt.

Magnetic hysteresis loops in Figure 4A,B show that the FePt NPs obtained from the annealing of the fcc-FePt/Fe_3O_4/MgO NPs at 600 and 650 °C for 6 h under Ar + H_2 (5%) are ferromagnetic. But the coercivity values of the FePt NPs from the 600 °C annealing are at 1.6 T (5 K), 1.2 T (100 K), and 0.4 T (300 K), much smaller than the FePt NPs from the 650 °C annealing at 3.2 T (5 K), 3.0 T (100 K), and 2.0

(28) Maeda, T.; Kai, T.; Kikitsu, A.; Nagase, T.; Akiyama, J. *Appl. Phys. Lett.* **2002**, *80*, 2147–2149.
(29) Kai, T.; Maeda, T.; Kikitsu, A.; Akiyama, J.; Nagase, T.; Kishi, T. *J. Appl. Phys.* **2004**, *95*, 609–612.
(30) Sun, X.; Kang, S.; Harrell, J. W.; Nikles, D. E.; Dai, Z. R.; Li, J.; Wang, Z. L. *J. Appl. Phys.* **2003**, *93*, 7337–7339.
(31) Takahashi, Y. K.; Ohnuma, M.; Hono, K. *J. Magn. Magn. Mater.* **2002**, *246*, 259–265.
(32) Kang, S. S.; Nikles, D. E.; Harrell, J. W. *J. Appl. Phys.* **2003**, *93*, 7178–7180.
(33) Kang, S. S.; Jia, Z.; Nikles, D. E.; Harrell, J. W. *IEEE Trans. Magn.* **2003**, *39*, 2753–2757.
(34) Jia, Z.; Kang, S. S.; Nikles, D. E.; Harrell, J. W. *IEEE Trans. Magn.* **2005**, *41*, 3385–3387.
(35) Yan, Q.; Kim, T.; Purkayastha, A.; Ganesan, P. G.; Shima, M.; Ramanath, G. *Adv. Mater.* **2005**, *17*, 2233–2237.
(36) Harrell, J. W.; Nikles, D. E.; Kang, S. S.; Sun, X. C.; Jia, Z.; Shi, S.; Lawson, J.; Thompson, G. B.; Sricastava, C.; Seetala, N. V. *Scr. Mater.* **2005**, *53*, 411–416.
(37) Tomou, A.; Panagiotopoulos, I.; Gournis, D.; Kooi, B. *J. Appl. Phys.* **2007**, *102*, 023910.
(38) Gersten, J. I.; Smith, F. W. *The Physics and Chemistry of Materials*; Wiley-Interscience: New York, 2001.

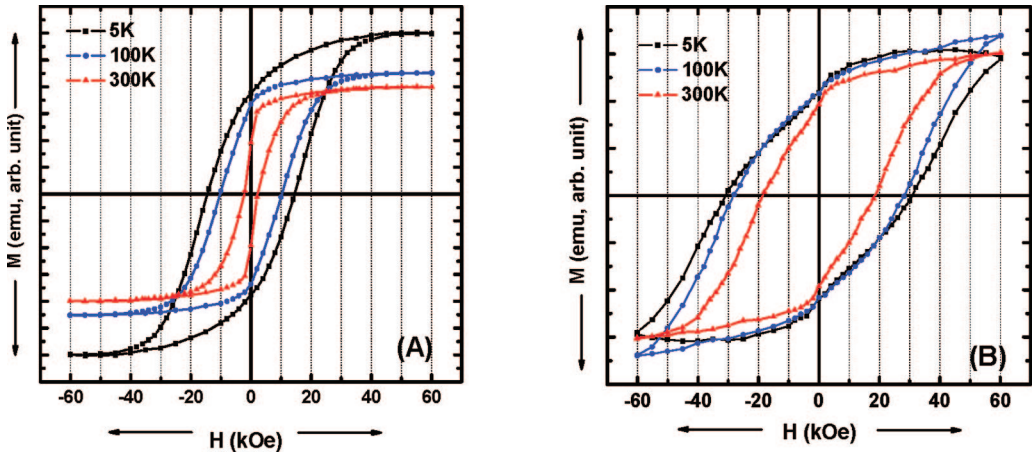

Figure 4. Hysteresis loops of the FePt/MgO NPs obtained after the thermal annealing of the FePt/Fe_3O_4/MgO NPs at (A) 600 °C and (B) 650 °C for 6 h under Ar + H_2 (5%).

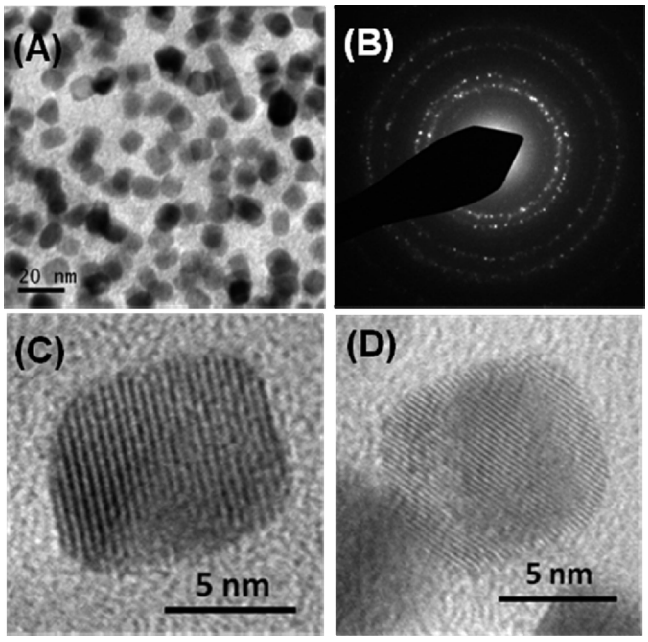

Figure 5. (A) TEM image of the fct-FePt NPs from their hexane dispersion; (B) SAED of the fct-FePt NP assembly in (A); and HRTEM images of the fct-FePt NPs with the lattices seen from (C) the (001) and (D) the (111) planes in fct-FePt.

T (300 K). More importantly, the magnetization values for the 650 °C annealed sample show little temperature dependence (Figure 4B). This indicates that the fct structure with large magnetocrystalline anisotropy in the 650 °C annealed FePt NPs is better formed. As a comparison, the FePt/MgO NPs annealed under the same 650 °C annealing conditions are superparamagnetic at room temperature.[17,27]

Dispersion and Characterization of fct-FePt NPs. The MgO shell in the fct-FePt/MgO NPs can be easily removed by diluted HCl (<10 vol %) washing and hexane extraction in the presence of HDT and OA, as reported before.[17] The TEM image of the fct-FePt NPs (Figure 5A) shows the isolated NPs that have little morphology change compared to the NPs seen in Figure 2. Figure 5B is the selected area electron diffraction (SAED) pattern of the fct-FePt NPs shown in Figure 5A. The ring patterns are from the fct-structured FePt NPs with the (001), (111), and (200) rings clearly visible in the inner circle. Figure 5C,D is two representative HRTEM images of the fct-FePt NPs. In Figure 5C, the lattice fringe spacing is measured to be 0.383 nm, corresponding to the (001) planes (0.384 nm spacing) in the fct-FePt. The FePt NP in Figure 5D has a lattice spacing of 0.224 nm, close to that of the (111) planes (0.222 nm spacing) in the fct-FePt. Magnetic measurements of these NPs show the similar hysteresis behavior to that in Figure 4B.

Conclusions

This report demonstrates an improved synthesis of ferromagnetic fct-FePt NPs and their dispersion from the Pt-rich fcc-FePt/Fe_3O_4/MgO NPs. The Pt-rich fcc-FePt/Fe_3O_4 NPs are made by a one-pot reaction of $Pt(acac)_2$ with $Fe(CO)_5$ in the presence of oleic acid and oleylamine and are coated with a layer of MgO via the thermal decomposition of $Mg(acac)_2$. The robust MgO coating prevents FePt NPs from sintering at high temperature reductive annealing conditions, and the core/shell structured FePt/Fe_3O_4 facilitates the fcc to fct conversion. The fct-FePt NPs show the coercivity values at 3.2 T at 5 K and 2 T at 300 K. These hard magnetic NPs can be stabilized by hexadecanethiol/oleic acid and dispersed in hexane. The synthetic strategy developed here is not limited to the FePt NP system but can be extended to the synthesis of other hard magnetic NPs of CoPt and $SmCo_5$ as well. With the size, composition, structure, and stability control, these ferromagnetic NPs can act as the key components in 2D or 3D magnetic NP superlattice arrays for nanomagnetism studies and for ultrahigh density magnetic information storage. The FePt NPs made by removing MgO in the absence of surfactant should be chemically active for various catalytic applications.

Acknowledgment. The work was supported by ONR/MURI under Grants N00014-05-1-0497, INSIC, and a GAANN fellowship to Y.L. We thank Mr. A. McCormick of Brown University for the HRTEM studies.

Supporting Information Available: EDS analysis and TEM images (PDF). This material is available free of charge via the Internet at http://pubs.acs.org.

CM8024878